

PREDICTING PARTICULATE MATTER EMISSIONS FROM SPRAY GUIDED GASOLINE DIRECT INJECTION SPARK IGNITION ENGINES

F Leach¹, R Stone

Department of Engineering Science, University of Oxford, UK

D Fennell, D Hayden, D Richardson, N Wicks

Powertrain Research, Jaguar Land Rover, UK

Abstract

An index, linking fuel composition with Particulate Matter (PM) emissions (PN index) has been developed and is here evaluated with model fuels in a single cylinder, optical access, Spray Guided Direct Injection (SGDI) engine; the model fuels having independent control of the double bond content and volatility, as used in the index. This index is investigated on three different engines: a single cylinder research engine, a V8 engine recently available in the market, and a current production supercharged V6 engine. A number of market gasolines have been tested across all three engines and all of the results follow the trends predicted by the PN index. Imaging of in-cylinder sprays shows the composition of model fuels affects the mixture homogeneity and their PM emissions; in particular the lack of a light-end in the model fuel composition can lead to misleadingly low PN emissions due to improved mixture preparation unrepresentative of market fuels. The index has been investigated in a Jaguar Land Rover V6 engine with five different fuels over a simulated NEDC and the results show the index trends are followed. Emissions have been evaluated from two fuels representing the EU5 reference-fuel specification that have been developed using the PN index to give a difference in PM emissions. The results from these fuels show that a difference in PN emissions of around a factor of two can be seen at both stoichiometric and rich conditions, for two fuels representative of the EU5 reference-fuel specification. This follows trends predicted by the PN index. This has important implications for policy makers

¹ Corresponding author: felix.leach@eng.ox.ac.uk

and EU legislation, where PN emissions from gasoline vehicles will be regulated for the first time, as batch to batch variations in fuel composition would result in differing test results under the current legislation.

Keywords

Particulate Matter, Emissions, Spray Guided Gasoline Direct Injection, Gasoline Direct Injection, Fuel Effects

Introduction

Gasoline Direct Injection (GDI) engines have become the standard for premium gasoline vehicles in many markets, replacing Port Fuel Injected (PFI) engines due to their lower specific fuel consumption, greater specific output, and lower CO₂ emissions. GDI engines emit more Particulate Matter (PM) than PFI engines¹, and without optimisation for reduced particulate emissions, modern GDI engines might not meet increasingly stringent EU emissions legislation². European emissions legislation, EU6 – effective 1 September 2014, mandates a particle limit of 6x10¹¹ #/km (with derogation to 6x10¹² #/km permitted for 3 years)³.

It is not surprising that different fuels have different levels of particulate matter emissions, and it is almost inevitable that even a single engine will not always be tested with the same fuel. So when comparisons are made between tests using different fuels, it would be useful to have a particulate matter index that enables a correction to be made based on the key fuel properties.

Aikawa et al⁴ conducted tests with a PFI engine and developed a model linking fuel composition with PM emissions. It links PM emissions with the Vapour Pressure (*VP*) and Double Bond Equivalent (*DBE*) of the components in the fuel weighted by their Mass Fraction (*W_i*):

$$PM\ index = \sum_{i=1}^n \left[\frac{DBE_i + 1}{VP_i} \right] W_{ti} \quad (1)$$

DBE is a measure of how unsaturated a hydrocarbon is, and can be easily calculated from:

$$DBE = \frac{2C - H + 2}{2} \quad (2)$$

Where *C* and *H* are the number of Carbon and Hydrogen atoms respectively present in an organic compound. As an example, toluene (methyl benzene, C₆H₅.CH₃) has a *DBE* of 4 as the corresponding saturated compound would be heptane (C₇H₁₆), which has a *DBE* of 0. The Vapour Pressure (*VP*) is evaluated at 443 K by means of an empirical correlation.

It should also be noted that Aikawa et al⁴ evaluated the vapour pressure at a range of temperatures, and found that a temperature of 443 K gave the best correlation between particulate emissions and the PM index. The vapour pressure was not a direct measurement, but came from an empirical relation between the normal boiling point of each component and its vapour pressure at 443 K. Aikawa et al found a strong correlation between their calculated PM index and measured particulate emissions (Figure 1) but there is insufficient compositional information of their fuels available in Aikawa et al⁴ for the PM index to be calculated independently.

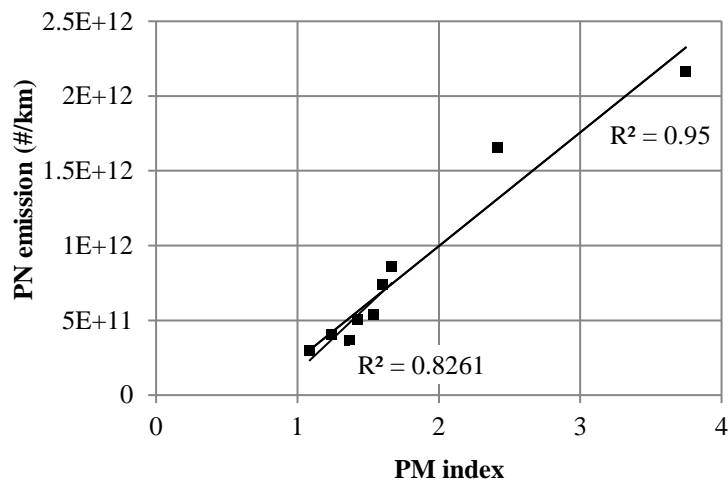


Figure 1: Relationship between PN (#/km) and PM index over NEDC (data from Aikawa et al⁴), different correlations are seen depending on whether or not the two fuels with the highest PM index are excluded

The work undertaken in Aikawa et al⁴ used a Port Fuel Injection (PFI) engine, and had no independent control of the fuel vapour pressure or DBE as commercial gasolines were used, along with a base fuel to which different components were added. Indolene was used as a base fuel, to which were added 10% by mass of components such as 2,2,4-trimethylpentane, dodecane, ethylbenzene, and 1,2,4-trimethylbenzene. The PM index range of the fuels tested was 1.01 – 3.86 and the index range of over 1,400 worldwide fuels available was calculated and can be seen in Figure 2. Figure 2 shows a very broad range of the PM index for these worldwide fuels, with a mean of 2.12 and a standard deviation of 0.81.

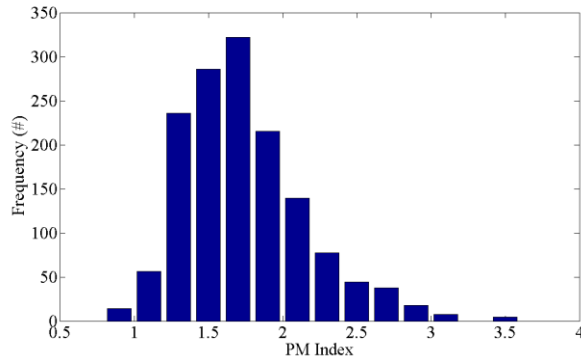


Figure 2: Range of PM indexes of a selection of commercially available fuels worldwide (data from Aikawa et al⁴)

A paper developing the PM index concept by two of the same authors of the original paper - Aikawa and Jetter⁵ – analyses the PM emissions (both mass and number) using 10 different commercial fuels from a 2.4 L wall guided GDI engine vehicle over the FTP75 cycle with PN measured according to the legislatively compliant PMP method⁶ with an EEPS in parallel for particle size data. Again calculation of the PM index required a full (and expensive) detailed hydrocarbon analysis.

Similar to the previous work, Aikawa and Jetter report a close agreement between their PM index and the overall PM emissions over a weighted FTP75 cycle; this can be seen in Figure 3. However they also report that the correlation between the PM index and the PM emission decreases significantly for Phase 2 (transient phase - more highway style driving) and Phase 3 (hot-start phase) compared with Phase 1 (cold start phase). This suggests that perhaps their PM index is only valid for cold start, and that the relative weighting of the VP in their index accounts for this, although, as Aikawa and Jetter say, the lower overall PN expected from Phase 2 and 3 and hence worse Signal to Noise Ratio (SNR) from the instrumentation may also account for this.

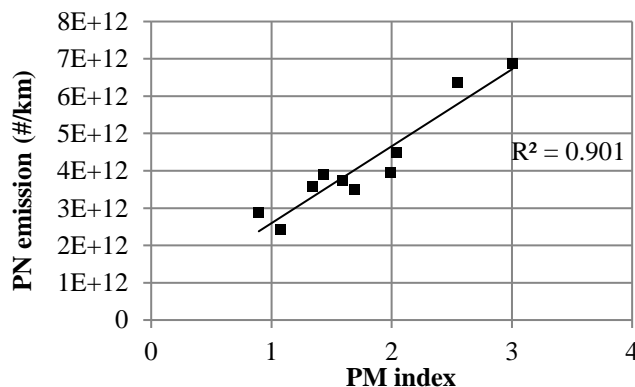


Figure 3: Relationship between PN (#/km) and PM index over FTP75 (weighted) (data from Aikawa and Jetter⁵)

For the (Aikawa) PM index a detailed Hydrocarbon Analysis (DHA) of fuels using a chromatographic method to provide a complete compositional breakdown by mass of the 200-300 hydrocarbons present in a typical gasoline is required. It is an expensive test, and not typically performed for gasoline. A DHA is necessary as each of the components is evaluated individually then incorporated into the index as a linear sum. The vapour pressure for mixtures of hydrocarbons does not behave as a linear combination of their values, and the method used by Aikawa et al⁴ does not take this non-linear behaviour into account.

Experimental methodology

Given the information on fuel composition that is typically available, it is possible to adapt the PM index by making changes such that a new index for fuels can be calculated without expensive, and time consuming extra analysis. This has obvious advantages. The industry standard is that fuels are blended by volume fraction; this is a small adaptation from the mass fraction used in the PM index. Parameters that can be used to calculate the DBE are included on a typical specification sheet; these are the aromatic content (DBE = 4), olefin content (DBE = 1), oxygenate content (DBE = 0), and paraffin content (DBE = 0), and a measure of vapour pressure – Dry Vapour Pressure Equivalent (DVPE) or Reid Vapour Pressure (RVP). DBE + 1 is used to ensure that the effect of components with a DBE = 0 is counted, for example combusting pure isooctane will still give PN emissions.

With this in mind a new index, the PN index is introduced, with the vapour pressure being evaluated as DVPE with units of kPa and the use of volume fraction (V_i) of each hydrocarbon group. The PN index is shown in Equation 3.

$$\text{PN index} = \frac{\sum_{i=1}^n [\text{DBE}_i + 1] V_i}{\text{DVPE (kPa)}} \quad (3)$$

DVPE was used as the measure of vapour pressure since this is a European standard measurement, which is evaluated at 310.95 K and the index has always been calculated here by volume fractions; an industry standard for fuel blending. The PN index is of course not an exact quantity, and a potential error can be calculated on it, by cascading down the reproducibility from the appropriate test methods (specified in the EU5 emissions legislation⁷), and assuming a ‘worst-case’ effect of each of the errors. The resulting errors have been plotted as bars on the displayed PN index in Figures 17, 18, 20, and 21.

The aim of this work is to review this index by independently controlling the volatility and double bond equivalent content of a fuel referenced to the Particle Number (PN) measurements from a modern Spray Guided Direct Injection (SGDI) combustion system.

The work described in this paper is split into three phases. The first, conducted on the single cylinder engine, was conducted at steady state, light load (1500 rpm, 2 bar BMEP); the second on the V8 at steady state, light load (also 1500 rpm, 2 bar BMEP), and the third on the V6 over a simulated New European Drive Cycle (NEDC). It should be stressed that the latter tests were performed with the engine on a transient test bed and the particulate emissions were sampled directly from the exhaust, down-stream of the catalyst, so was not a legally compliant test, as it was not performed with a vehicle on a chassis dynamometer, or with the specified particle sampling procedure.

Engines

GDI engines are becoming very widely used in Europe, with either a central injector (Spray Guided Direct Injection - SGDI) or a side mounted injector. The engine for the model and reference fuel work is a single-cylinder SGDI engine with optical access supplied by Jaguar Land Rover. The combustion system is based on the Jaguar AJ133 V8 engine. A solid model view of the combustion system is shown in Figure 4.

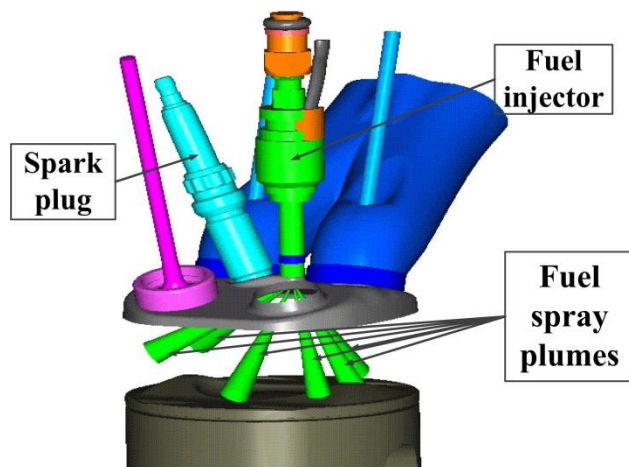


Figure 4: Solid model of the Jaguar AJ133 combustion system (adapted from Sandford et al⁸)

As shown in Figure 4, the injector delivers six spray plumes, four down into the cylinder and two plumes, which straddle the spark plug. The emission levels of SGDI type engines have the potential to meet the forthcoming particulate number emissions legislation, but as reported elsewhere the exact level would be very dependent on the warm-up strategy and any rich mixture excursions during accelerations².

The second column of Table 1 shows the engine specification. This engine is not fitted with a catalyst. A lambda sensor was used to measure oxygen content in the exhaust and to set the correct fuel injection pulse width to achieve the mixture stoichiometry required for the test, either nominal stoichiometric ($\lambda=1.01$) or 10% rich ($\lambda=0.9$). As slight rich mixture excursions have a large effect on particulate emissions⁹, a lambda of 1.01 was chosen to avoid these.

The AJ133 5.0 L naturally aspirated V8 engine was used for steady state testing of the PN index. The engine has been fully described by Sandford et al⁸. The engine is fitted with a three-way-catalyst (TWC), on each bank of four cylinders. It is expected that the TWC will act to remove the nucleation mode particles from the exhaust, leaving the accumulation mode largely unchanged¹⁰. The specifications of the engine are show in the third column of Table 1.

The drive cycle work was performed on an AJ126 3.0 L V6 supercharged engine. The AJ126 is based on the AJ133 V8 technology⁹; the quad-cam V6 shares its all-aluminium construction with the AJ133. The supercharger is mounted in the 'V' of the engine and is a Roots-type twin vortex supercharger. The engine is fitted with a water-cooled intercooler, and Bosch engine management software. The engine was fitted with a standard TWC on each engine bank. The fourth column of Table 1 shows the engine specification.

For the AJ126 experiments the engine was mounted on a transient dynamometer set to run a simulated cold-start NEDC. The engine was loaded as a Sports Utility Vehicle (or similar) and stop-start operation was enabled.

Table 1: Engine specifications

Engine	Single cylinder with optical access	AJ133 V8	AJ126 V6
Bore × Stroke	89× 90.3 mm	92.5× 93.0 mm	84.5× 89.0 mm
Displacement	562 cm ³	4999 cm ³	2995 cm ³
Valves per cylinder	2 intake, 2 exhaust	2 intake, 2 exhaust	2 intake, 2 exhaust
Compression ratio	11.1 : 1	11.5 : 1	10.5 : 1
Fuel pressure	150 bar	150 bar	150 bar
Aspiration	Naturally aspirated	Naturally aspirated	Supercharged

Instrumentation

Two particulate measurement instruments have been used. A Cambustion DMS500 (DMS), and an AVL Particle Counter (APC). The DMS uses electrical mobility measurements of particles to give particle size, number and mass; it is fully described in Reavell et al¹¹. A previous study² has shown that using the accumulation mode particle number from the DMS500 agrees very well with a Particle Measurement Programme (PMP) compliant solid particle counting system⁷ (SPCS) that effectively discounts nucleation mode

particles. In accordance with this, only the accumulation mode output of the DMS was used. The correlation between DMS data and a legally compliant PMP test from earlier work can be seen in Figure 5².

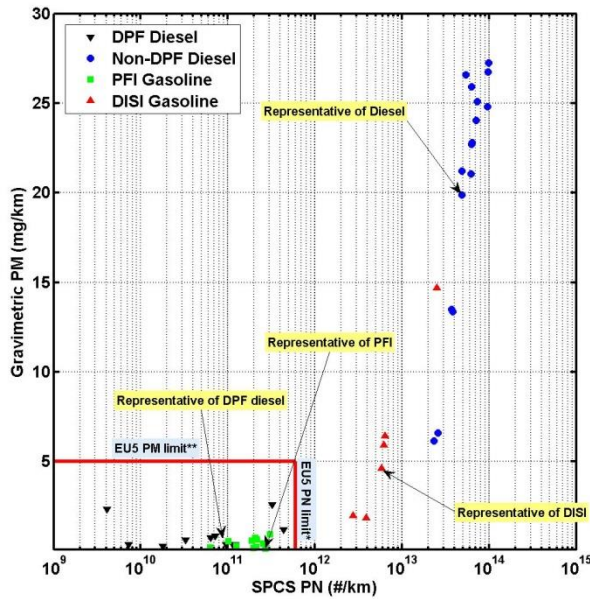


Figure 5: DMS500 PN result plotted against regulation-compliant SPCS PN result. For these data points, the DMS500 sampled directly from the vehicle tailpipe from Braisher¹²

The APC is a condensation particle counter, only giving particle number, it is fully described in Giechaskiel et al¹³, and it can be used as part of a legally compliant counter. The sampling point for both particle measuring instruments was in the centre of the exhaust flow, several metres downstream of the exhaust valves, and (in the case of the V8 and V6) post-catalyst. For the steady state measurements a sample of at least 90 s was taken, and averaged. The NEDC experiments were run three times and averaged.

In-cylinder Hydrocarbon (HC) levels were measured in the single cylinder engine using a Cambustion HFR400 fFID¹⁴, which measures hydrocarbon levels by chemi-ionization. For this experiment the hydrocarbon sample was taken at the circumference of the cylinder, approximately 10 mm below the cylinder head. The system response time was around 4 ms, which corresponds to 36 CA at 1500 rpm.

A Photron FASTCAM-1024PCI model 100K colour camera was used to record the injection and combustion images in the single cylinder optical access engine at a rate of 6000 frames per second (fps), which corresponds to 1 frame per 1.5° crank angle at 1500 rpm. At this frame rate a resolution of up to 512×256 or 384×368 pixels was available. The fuel spray was illuminated using a green LED array, pulsed synchronously with the spray and over-driven to provide sufficient illumination.

The transient dynamometer used for the V6 tests was controlled by a ‘turn-key’ CP Engineering system.

Design of the model fuels

The aim of the model fuels was to be able to vary a fuel’s DBE and VP independently, while ensuring that the individual components of the fuels coevaporated on injection, such that there were no areas of the mixture rich in a particular component. The model fuel design was also limited by octane number (the test engine at the test condition could run with a RON of 70). The model fuels have been designed using an evaporation model, octane number considerations, and knowledge of component DBE.

Evaporation modelling

The simplest model for evaporation uses the Raoult-Dalton law¹⁵, commonly known as Raoult’s law. Raoult’s law relates the vapour pressure of an ideal solution to the vapour pressure of each of its chemical components by the molar fraction of each component present.

$$y_i P = x_i P_{vpi} \quad (4)$$

Here y_i is the molar fraction of component i in vapour, x_i is the molar fraction of component i in liquid, P_{vpi} is the vapour pressure of component i , P is the pressure of the mixture.

Raoult’s law assumes ideal mixture behaviour, which gives Raoult’s law its linear relationship. Mixtures of aromatics and paraffins are not ideal¹⁶ so to model them Raoult’s law has to be modified by methods such as UNIFAC.

UNIFAC provides temperature-dependent activity coefficients (γ_i), which modify Raoult’s Law:

$$y_i P = \gamma_i x_i P_{vpi} \quad (5)$$

To validate this model, a distillation curve of a known fuel was modelled. The results in Figure 6 show that the UNIFAC model follows the distillation curve closely, with the exception of the beginning and end of the distillation, which can be attributed to distillation equipment artefacts.

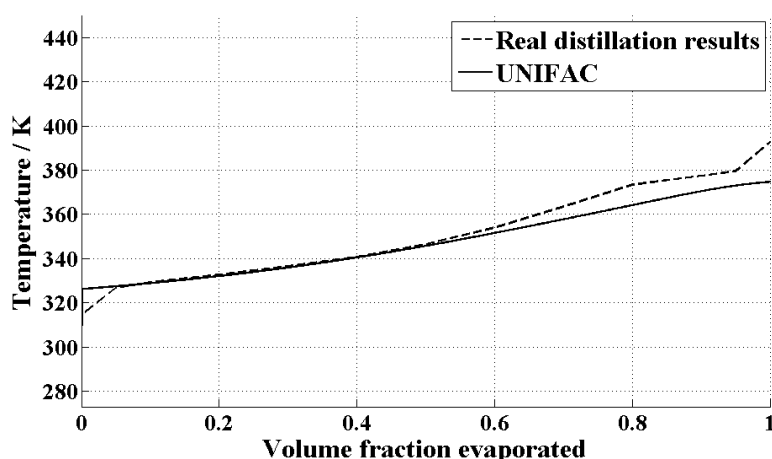


Figure 6: Comparison between UNIFAC model and real distillation of ULG

The UNIFAC extension to Raoult's Law¹⁷ has been used to design fuels in which the components in either the medium or low volatility fractions of the model fuels co-evaporate. The method is described in Appendix 2 and the resulting fuel compositions are in Appendix 2.

The results of the model are shown in Figure 7 and Figure 8 (here 'T' blends refer to fuels whose label starts with a 'T' and are varying DBE, and 'D' blends refer to fuels whose label starts with a 'D' and are varying volatility). These are plotted such that perfect coevaporation of aromatic and paraffin components is indicated by a straight line at unity on the ordinate. Understanding what the model is predicting is easy to see in the results of the T100 fuel in Figure 7, a mixture (by volume) of 95 % toluene and 5 % n-pentane², where the more volatile n-pentane evaporates more quickly initially, in preference to the toluene, before the toluene 'catches up' for the rest of the evaporation. These results were used to set iso-octane : n-octane and iso-decane : n-decane ratios alongside the octane number which is discussed in the fuels section.

² The initial nomenclature for the model fuels was developed before it was decided to add 5 % (v/v) n-pentane to all of the fuels; hence T100 is not 100 % toluene, rather a 95 % toluene, 5 % n-pentane mixture.

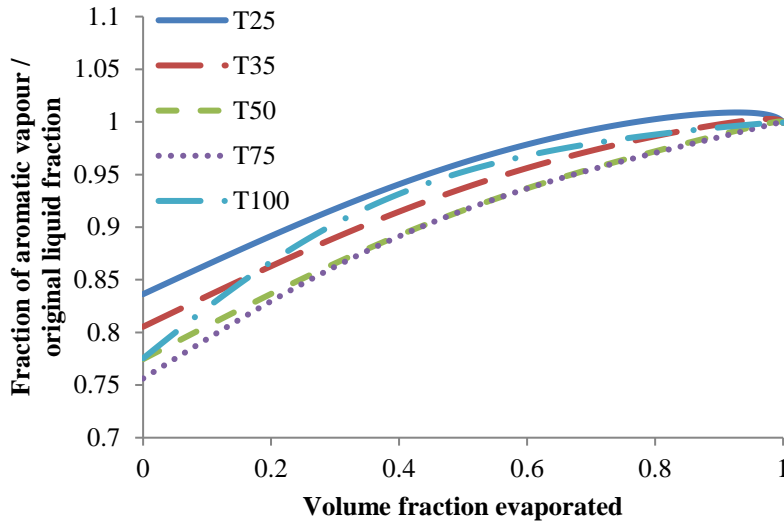


Figure 7: UNIFAC model results on 'T' blends, there is little difference between the fuel blends, and only small differences in paraffin to aromatic ratio can be seen

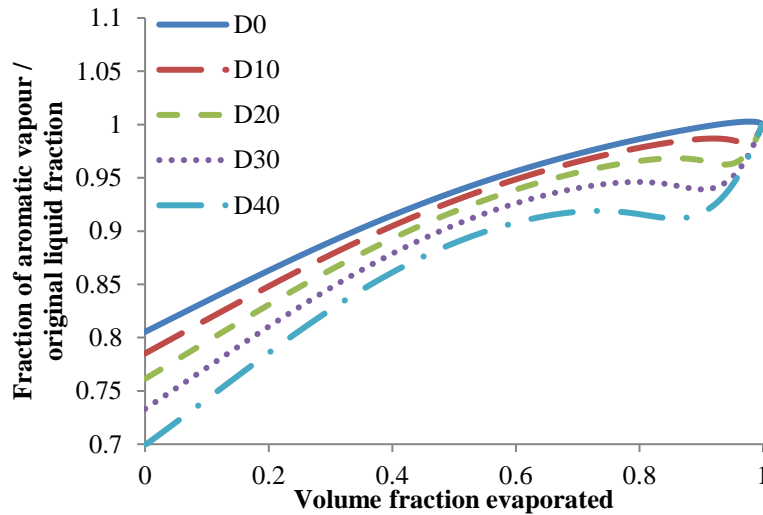


Figure 8: UNIFAC model results on 'D' blends, again there are few differences between the fuel blends, and only small variations in paraffin to aromatic ratio can be seen

The vapour pressure of gasoline is measured in accordance with EN 13016-1¹⁸ and is expressed as Dry Vapour Pressure Equivalent (DVPE), (and an equivalent US standard is Reid Vapour Pressure (RVP)). This standard uses a temperature of 37.8 °C (310.95 K), whereas the PM index in Aikawa et al⁴ uses the absolute vapour pressure of the individual components of the fuel at a temperature of 443 K. DVPE is intended to be equivalent to RVP¹⁸, and is calculated from a statistical correlation equation to give a dry Reid Vapour Pressure. Another common measure of vapour pressure is the Air Saturated Vapour Pressure (ASVP). The differences

between Reid Vapour Pressure, DVPE and ASVP, are all small (and comparable to uncertainties when they are measured or modelled); they are all essentially absolute vapour pressures.

DVPE can easily be converted to ASVP¹⁹:

$$DVPE(kPa) = (0.965ASVP(kPa)) - 3.78 \quad (6)$$

The difference between ASVP and VP comes from the dissolved air in the liquid in the ASVP test. This can be approximated from Henry's Law¹⁹:

$$p = k_h c \quad (7)$$

Here p is the partial pressure of the solute gas in solution, k_h is a temperature dependent coefficient, and c is the concentration of the solute. The Van't Hoff equations¹⁹ can be used to calculate k_h , and are temperature dependent. Henry's law can then be used to calculate the air dissolved in the liquid at 273.15 K that will come out of solution at 310.95 K. This provides an approximate conversion from VP to ASVP.

Aikawa et al⁴ show that the correlation coefficient between the PM index and Particle Number emissions is still 0.90 for an Absolute Vapour Pressure calculation temperature of 310.95 K. This is shown in Figure 9. Although this correlation is not as good as that at 443 K that Aikawa et al use, a value of 0.9 is still good, and VP at 310.95 K (whether RVP or DVPE) is the VP that appears on fuel data sheets so, for this reason, this was the calculation temperature chosen.

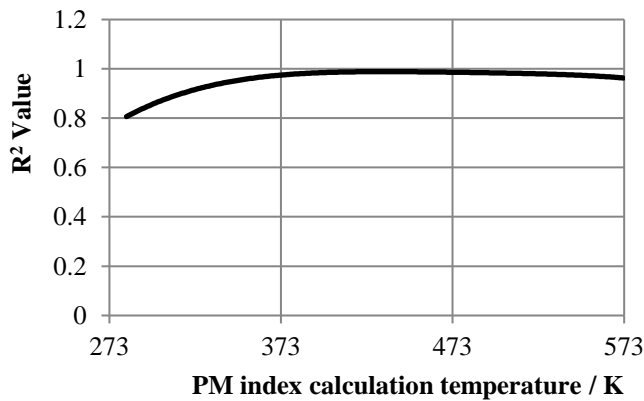


Figure 9: Fit of determination coefficient between Particle Number emissions and PM index for different Vapour Pressure evaluation temperatures (data from Aikawa et al⁴)

For the model fuels mixed from pure components, for which the complete compositional breakdown was known, but DVPE was not known, the PN index was calculated using VP calculated at 310.95 K (using the UNIFAC method discussed in Appendix 2) then converted to DVPE using Equations 6 and 7. For commercial gasolines, the stated DVPE or RVP was used.

Fuels

Model Fuels

Our target was to vary the DBE and VP independently with model fuels blended from pure components. Toluene and 1,3,5-trimethylbenzene were chosen as aromatic components having medium and high boiling points (both with a DBE of 4), and then their paraffin counterparts were selected on the basis of having adjacent boiling points, with blends selected to give co-evaporation with the corresponding aromatic component. Pentane was used to provide a volatile ‘front end’. When the volatility was varied, the aromatic content was kept at 35 %, as it is the upper limit for the aromatic content in European gasoline and it maintains the octane number above 70.

Ensuring mixture co-evaporation and homogeneity was a key goal throughout. This had to be balanced against the Research Octane Number (RON) of the fuel. Previous experiments have determined that at part load the minimum RON that this engine required was 70. This was a particular challenge as n-octane has a RON of -17; long straight-chain molecules coevaporate well with the aromatic components but have low RON values. The RON limit of 70 was key in choosing both the iso-octane : n-octane and iso-decane : n-decane ratios as well as setting the heavy component limit of 40 %. It can be seen from Figure 10 that this criteria was met, and the ratios chosen are: iso-octane : n-octane ratio 75:25 and iso-decane : n-decane ratio 24:76 (see Appendix 3).

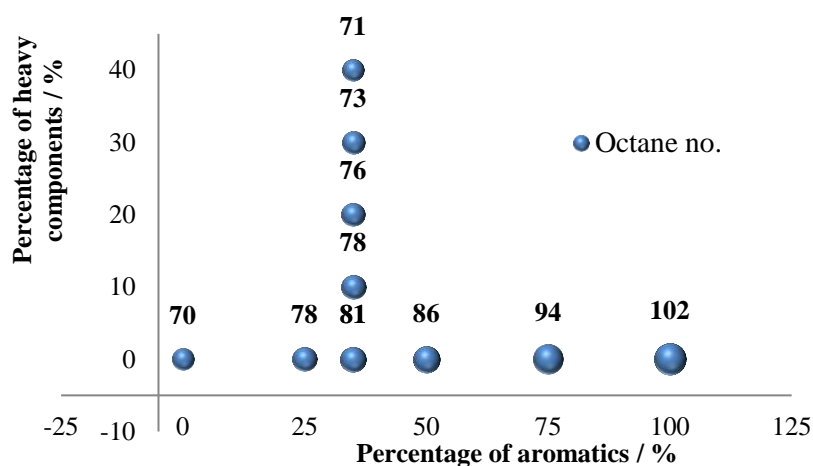


Figure 10: Research Octane Number (RON) and composition of the model fuels(calculated using Blending Octane Numbers of pure components)

The final composition for the model fuels (Appendix 3) shows that there is independent control over the double bond equivalent and vapour pressure of the fuel.

Commercial Fuels

Two fuels, which comply with EN228²⁰, the European standard for pump gasoline, have also been tested in the single cylinder engine. Their composition is detailed in Table 2. Testing the PN index using market fuels is an important part of its validation.

Table 2: EN228 compliant fuel compositions

	DBE+1 (% v/v)	DVPE (kPa)	PN index (1/kPa)
S070907	2.58	70.6	3.66
S103275	2.25	88.6	2.54

Reference Fuels

The Euro 5 emissions standard specifies a parameter range for the test fuel⁸, and the parameters relevant to the PN index can be seen in Table 3.

Table 3: CEC RF-02-08 Reference fuel specification ⁸ (compliant with EU5 emissions legislation)

	Min	Max
DVPE (kPa)	56.0	60.0
Olefins (% v/v)	3.0	13.0
Aromatics (% v/v)	29.0	35.0

These parameters can be arranged to give a maximum and minimum PN index possible with a reference fuel meeting the specification, as seen in Table 4. It can be seen that a large variation in the index is theoretically possible.

Table 4: Reference fuel parameters for greatest PN index variation

	Min PN index	Max PN index
DVPE (kPa)	60.0	56.0
DBE+1 (% v/v)	2.19	2.53
PN index (1/kPa)	3.65	4.51

It was decided to blend two fuels, which would meet the EU5 (CEC RF-02-08) reference fuel specification but with differing PN indices. The relevant parameters of their composition can be seen in Table 5. The blending process was unable to meet the volatility specification exactly, but the error is small, and these two fuels are certainly representative of the CEC RF-02-08 specification.

Table 5: CEC RF-02-08 representative test fuel composition

	DBE+1 (% v/v)	DVPE (kPa)	PN index (1/kPa)
Fuel A	2.20	61.7	3.56
Fuel B	2.49	59.9	4.16

Drive cycle test fuels

Five fuels with a spread of the PN index were selected for the drive cycle experiments. At both ends of the PN index, fuels were selected that had a low (or high) index due to either a high (or low) vapour pressure or DBE, giving some form of independent control over these parameters. The properties of these fuels are shown in Table 6. Of note from these fuels, Fuel 3 is compliant with the EU5 reference fuel specification and Fuel 5 is a Japanese TRIAS certification fuel.

Table 6: Drive cycle test fuel composition

	DBE+1 (% v/v)	VP* (kPa)	PN index (1/kPa)
Fuel 1	2.11	106.1	1.99
Fuel 2	1.98	92.9	2.15
Fuel 3	2.32	56.2	4.07
Fuel 4	2.28	47.8	4.77
Fuel 5	2.95	57.3	5.14

* either DVPE or RVP depending on fuel analysis method

Results and discussion

Here the PN index has been tested on three engines with several fuels. Model fuels, with independent control of double bond equivalent and vapour pressure, two EN228 compliant fuels, and two CEC RF-02-08 reference fuels have been tested on a single cylinder, optical access engine at light load, the two CEC RF-02-08 reference fuels have been tested on a V8 engine at steady state, light load, and five different fuels have been tested on a V6 engine, simulating a legislative test cycle, and the results compared to the PN index.

Model fuel results

For these experiments the engine was run at a fixed operating point shown in Table 7. The engine was run with open loop lambda control with a lambda of 0.9. This is to reflect the rich mixture excursions which are known to have a large effect on the particulate matter emissions²⁰.

Table 7: Single cylinder engine operating point

IMEP (bar)	1.8
Inlet air temperature (°C)	40
Coolant temperature (°C)	60
Lambda	0.9
RPM	1500
Start of ignition (°CA bTDC)	35
Start of Injection (°CA bTDC)	280

Results for model fuels tested in the single cylinder optical access engine are shown in Figure 11. It can be seen that the particulate number emission follows the trend of the index. Unfortunately the variation in PN index for fuels with fixed DBE and varying volatility is small, and as such the effects are difficult to discern amid the normal variations in particles emitted. Here the PN emissions were measured at steady state for a period of at least 90s, the error bars here represent one standard deviation, and show the variation in the levels of particulates emitted over this period.

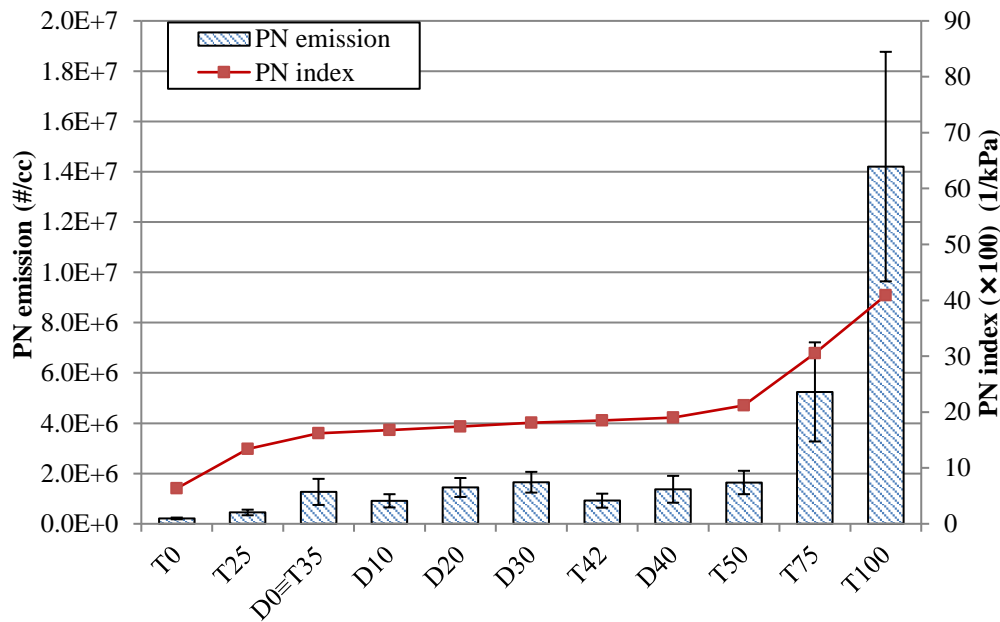


Figure 11: Particulate number emissions and PN index value variation for model fuels (independent control of DBE and VP , the error bars correspond to $\pm \sigma$ for the PN results

The results shown in Figure 11 have been plotted again in Figure 12, this time comparing the PM index and PN index value of each of these fuels, the PN emission is shown as proportional to the area of the ‘bubbles’ displayed (no error is plotted here for clarity, but the error can be seen on Figure 11). It can be clearly seen that the PN index appears to provide a better indication of the PN emission compared to the PM index, indeed two fuels with almost the same PN index, but very different PM indices, T42 (which has a PM index of 0.684 and a

PN index of 0.185) and D40 (which has a PM index of 1.31 and a PN index of 0.182), give almost the same PN emission (9.2×10^5 and 1.4×10^6 #/cc respectively), and not the factor of two difference predicted by the PM index.

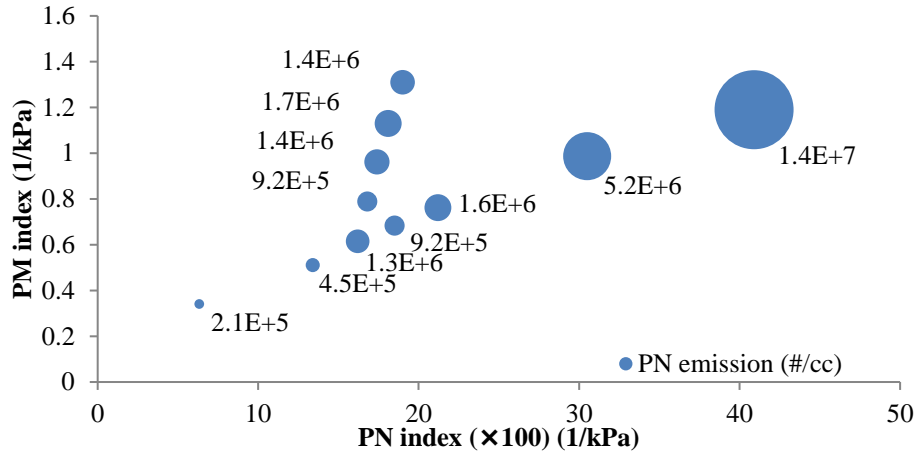


Figure 12: Comparison of PN index and PM index with the measured PN emission (represented by the ‘bubble’ size)

Spray image analysis and fFID results

The fuels used here all contain 5% n-pentane by volume, which is used to mimic the light end found in commercially available fuels. It can be shown that the presence of this light end is vital with fuels mixed from pure components in order that their evaporative performance, and hence PN emissions, are comparable with commercially available fuels.

Comparisons were run using identical fuels, with and without 5% n-pentane present. Figure 13 shows the evolution of the in-cylinder hydrocarbon levels, measured using a fFID, 10 mm below the cylinder head gasket on the cylinder liner. Measurements were taken over 69 cycles, and at each crank angle the average and standard deviation were calculated. The standard deviation was used to give an indication of the cycle-to-cycle variations. It can be seen that the hydrocarbon levels are significantly higher, and rise faster, when there is pentane in the fuel, indicating more rapid dispersion of the fuel in the cylinder, and that the cycle-to-cycle variations are higher. This suggests that the mixture is less homogeneous when pentane is present, indicating that the presence of pentane leads to a breaking-up of the spray sooner in the cylinder.

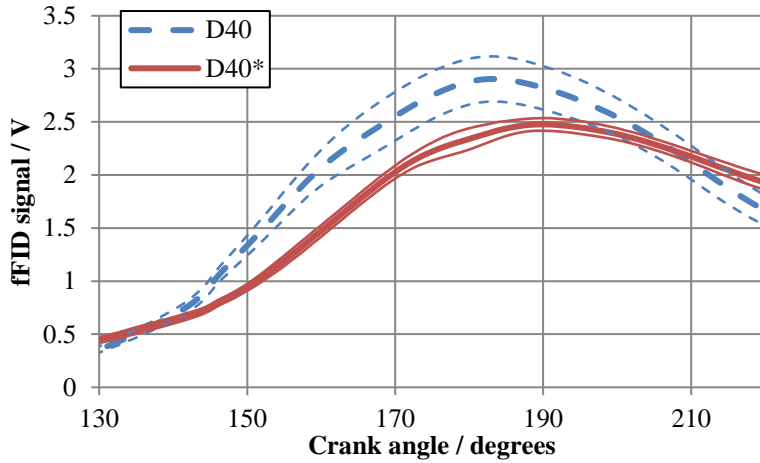


Figure 13: In-cylinder hydrocarbon levels for D40 (with *n*-pentane) and D40* (without *n*-pentane) sampled 10 mm below the cylinder head gasket and 45 °around from the front of the engine; the error bands (defined by the narrow lines) correspond to $\pm \sigma$

The hydrocarbon levels were sampled at different locations around the cylinder liner. Figure 14 shows that the pentane leads to greater variability and circumferential variation of the fFID signal. The smaller circumferential variation and cycle-to-cycle variations when there is no pentane suggests that the pentane reduces the homogeneity of the mixture.

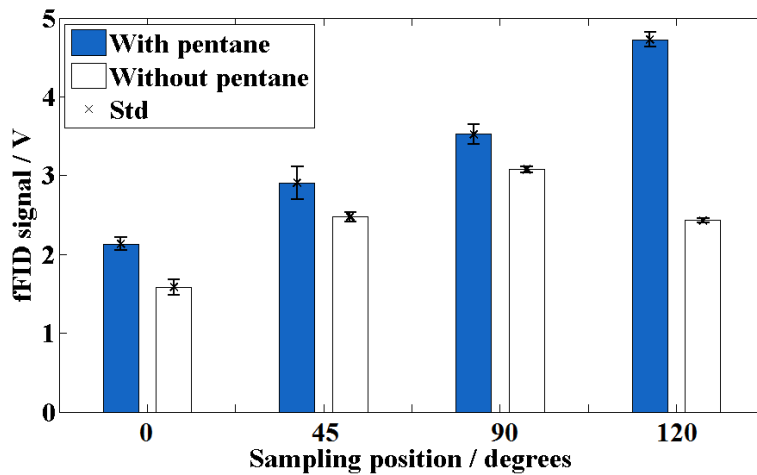


Figure 14: Effect of annular sampling position on the peak fFID signal for fuels with and without pentane; the standard deviation bars indicate the cycle-to-cycle variations in the mixture (0° is the front of the engine)

These observations about fuel dispersion are supported by looking at images of the fuel spray during injection. Figure 15 shows parallel sets of false coloured image of the fuel spray, on the left, D40 (which includes 5% v/v *n*-pentane) and, on the right, D40* (D40 without *n*-pentane). It can be seen that the presence of

n-pentane causes the fuel spray to break-up more quickly, whereas the fuel without n-pentane disperses further into the cylinder before evaporation, and this would account for the more homogeneous mixture. Whilst it is possible that an increase in fuel dispersion might increase spray impingement on the cylinder surfaces, our optical components showed no signs of such impingement nor the associated pool fires.

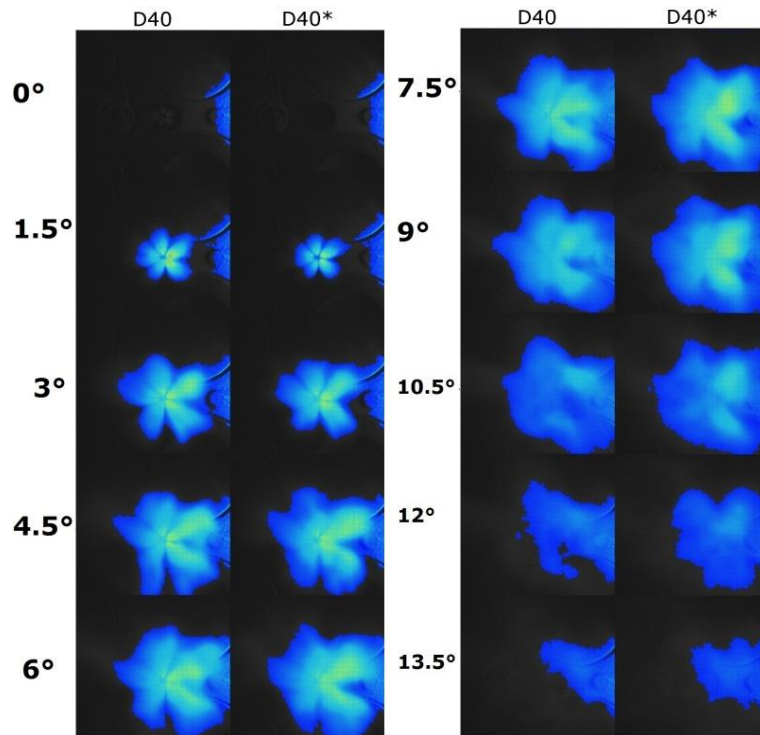


Figure 15: False colour images of the D40 fuel spray a) with pentane (D40) and b) without pentane (D40*), units of CAD after the start of injection

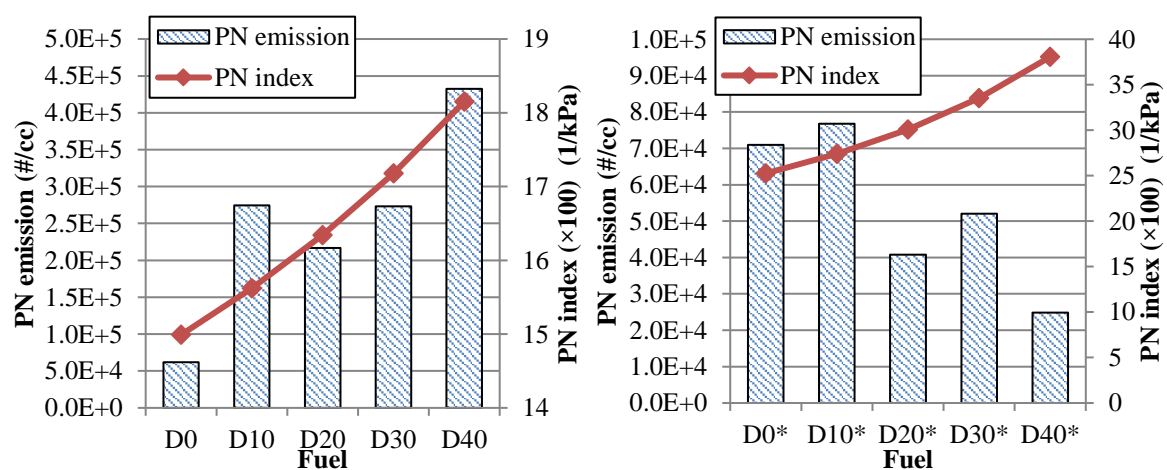


Figure 16: PN emissions compared with the PN index for D fuels a) with and b) without pentane. These results show the effect of adding 5% n-pentane causes the D fuels to behave as predicted by the PN index, rather than oppose the trends predicted by the index

The effect of not adding pentane on the mixture homogeneity is also seen in the particulate emission results. Figure 16 shows the PN emissions (in $\#/cm^3$) for the set of fuels with a constant DBE (again fixed at a 35% aromatic content) but without 5% pentane added. Figure 16b shows that as the vapour pressure of the fuel is decreased (with fixed DBE), the level of the PN emissions also decreases, due to the increased mixture homogeneity. This trend is the opposite to that predicted by the PN index, and shows the importance of adding high vapour pressure components, in small quantities, to make model fuels mixed from pure components more representative of commercial gasoline.

EN228 compliant fuel results in the single cylinder engine

Figure 17 shows the PN emissions (in $\#/cm^3$) for two fuels that meet the EN228 specification²⁰. Figure 17 shows that, for both stoichiometric and rich operation, the trends of the PN index are reflected in the PN emissions of these commercially available gasolines, indeed the PN index appears to under predict the change in PN emissions. This result, that the PN index is a good indicator of PN emissions from this engine, led to an increased interest in the PN index, and the further applications detailed in this paper.

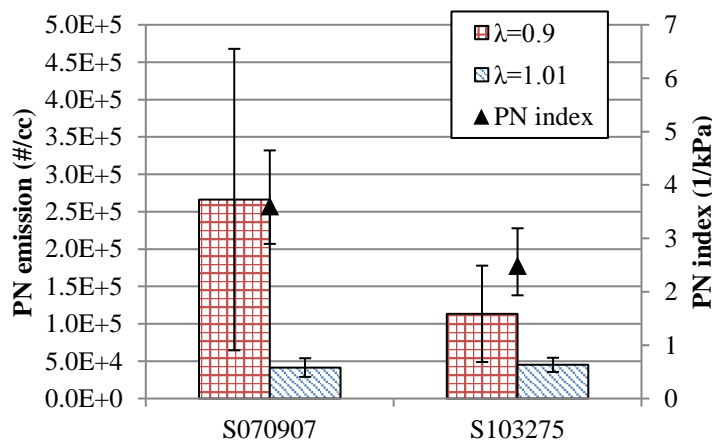


Figure 17: PN emissions from two EN228 compliant fuels, the error bars correspond to $\pm \sigma$ for the PN results and maximum error on the PN index (as calculated from the reproducibility of the test methods)

Drive cycle results

The results of the V6 drive cycle tests are shown in Figure 18. Each fuel was tested three times; with Fuel 3 being the first fuel tested (three times), and then repeated at the end a further three times. It can be seen that the repeat of Fuel 3 has given a highly repeatable result; giving reassurance that no drift effects have been present. It can be seen that there is some impact of the PN index, but much less than was predicted. This is

reinforced in Figure 19, where the PN emission is plotted against the PN index; the correlations between the total emission and the index are relatively flat, although the PN index still has an influence.

Breaking the cycle down into its constituent parts however reveals more detail. Here, the first 100 s of the cycle is referred to as the ‘Cold start’, 100-800 s as the ‘Urban’, and 800-1180 s as ‘Extra Urban’. Fuel 4 has the lowest VP of all the fuels, and so will take the longest to evaporate upon injection. Fuel 4 also has the highest emission in the Extra Urban portion of the cycle, which requires the highest load from the engine, suggesting perhaps that some spray impingement is taking place – leading to higher PN emissions. Likewise the Urban portion of the cycle correlates better with the DBE of the fuel, Fuel 5 having the highest DBE, and the highest Urban emission. The Cold Start part of the cycle again seems to correlate best with VP, unsurprising perhaps given the dependence of this part of the cycle on fuel evaporation. The cold start, and use of stop start, may also cause deviation from the results observed on the single cylinder optical access engine, which was run fully warm.

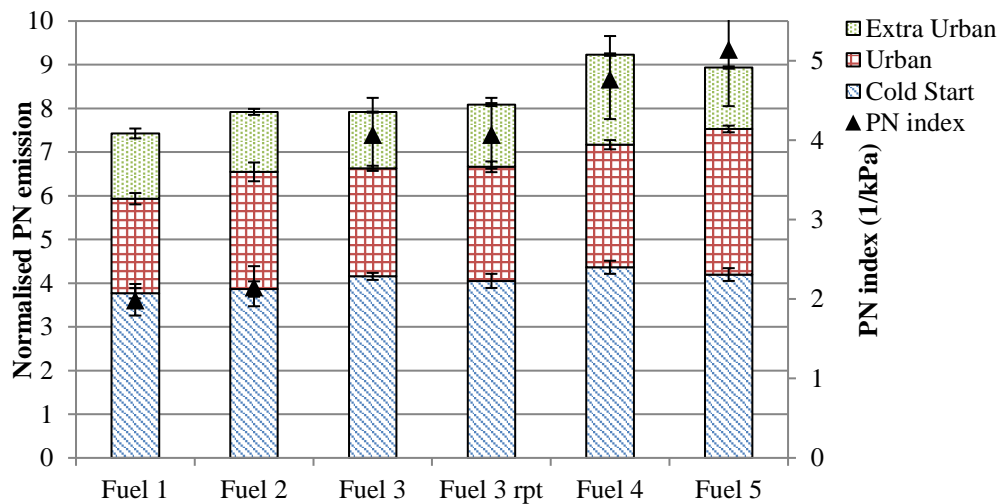


Figure 18: PN emissions over NEDC (APC results), the error bars correspond to $\pm \sigma$ for the PN results and maximum error on the PN index (as calculated from the reproducibility of the test methods)

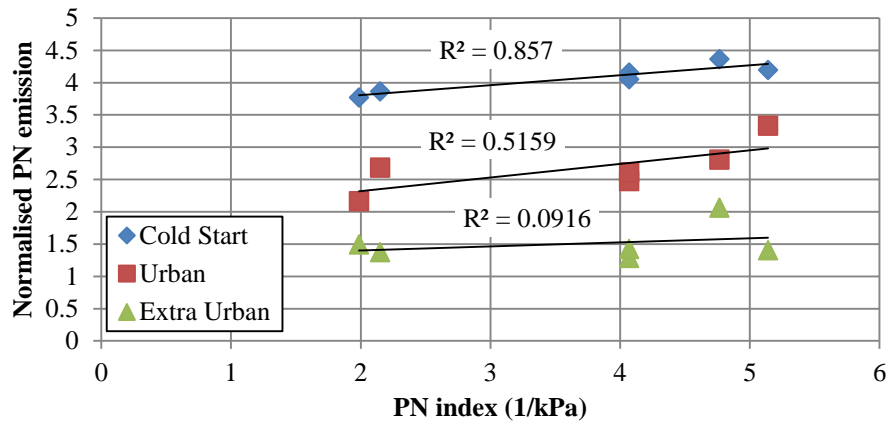


Figure 19: PN emission plotted against PN index (APC results)

Reference fuel results

Figure 20 shows the PN emissions (in $\#/cm^3$) from the single cylinder engine for two fuels which represent the reference fuel specification for testing against EU5 emissions legislation. It can be seen that the trends of the index are followed both at a stoichiometric and a rich condition, with a difference in PN emissions of around a factor of three (in fact greater than that predicted by the index).

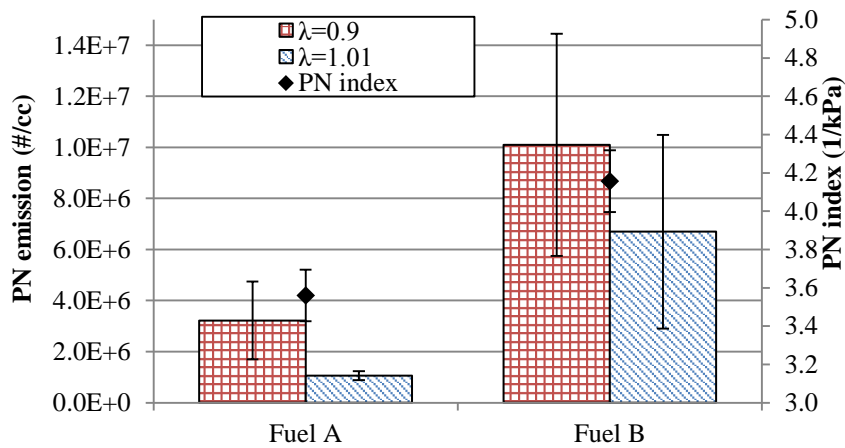


Figure 20: PN emissions from two fuels representing the EU5 Reference fuel specification in the single cylinder engine, the error bars correspond to $\pm \sigma$ for the PN results and maximum error on the PN index (as calculated from the reproducibility of the test methods)

For the V8 engine experiments the engine was run at a fixed operating point shown in

Table 8.

Table 8: V8 engine operating point

IMEP (bar)	1.8
Inlet air temperature (°C)	20
Coolant temperature (°C)	80
Lambda	1.0
RPM	1500

Figure 21 shows the PN emissions (in $\#/cm^3$) for two fuels which represent the reference fuel specification for testing against EU5 emissions legislation. It can be clearly seen that the PN emissions of the fuels follow the PN index.

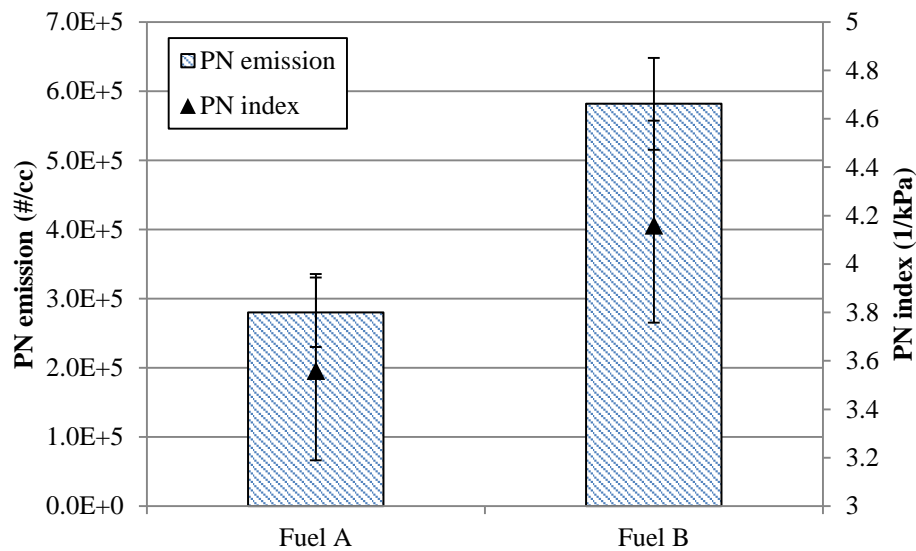


Figure 21: PN emissions from two fuels representing the EU5 Reference fuel specification in the V8 engine, the error bars correspond to $\pm \sigma$ for the PN results and maximum error on the PN index (as calculated from the reproducibility of the test methods)

A comparison of Figure 21 with Figure 20 shows that both engines have a difference in PN emission of around a factor of two, which is greater than that predicted by the PN index. Both of these results have important implications for the EU6 emissions legislation, where PN emissions from gasoline vehicles will be regulated for the first time. Unless the reference fuel specification is changed or an allowance is made for the

specific batch composition, then measured PN emissions during certification tests will vary depending on batch-to-batch fuel variations although the fuels meet the same specification.

Conclusions

A range of fuels has been tested on three different Spray Guided Direct Injection gasoline engines. The PN results from a single cylinder, optical access engine show that the PN index is a useful tool in predicting PN emissions. The PN index has been shown to give a better prediction of PN emissions from the single cylinder engine compared to the PM index developed in previous work, indeed two fuels with the same PN index, but a PM index differing by a factor of two, give the same PN emission.

Use of high speed imaging and fFIDs shows that evaporation of the model fuels is dependent on ‘light-end’ components – in this case 5% v/v n-pentane – being present in the fuel if they are to be representative of commercial fuels. Indeed both the fFID and high speed imaging data show that improved mixture homogeneity can lead to misleadingly low PN emissions for fuels without n-pentane present.

Results from a supercharged V6 engine over a drive cycle have shown that fuel composition is an important consideration when measuring PN emissions over an NEDC, but other factors can mask the effect of the PN index, in particular the cold start phase. In addition it has been seen that different parameters in the PN index have differing impacts on the PN emission from different parts of the NEDC, with fuel vapour pressure being an important consideration in the extra urban phase. The PN index has been shown to be an important parameter for fuel specification.

It has been shown that two fuels meeting the EU5 reference fuel specification can have differing PN emissions (of around a factor of two) at both stoichiometric and rich conditions, following trends predicted by the PN index. This has been demonstrated on both a single cylinder research engine and a V8 engine. This has important implications for policy makers and EU legislation where PN emissions from gasoline vehicles will be regulated for the first time as batch to batch variations in fuel composition would result in differing test results under current legislation.

Acknowledgments

The authors wish to thank David Richardson and Coryton Fuels for supplying the specially blended CEC RF-02-08 reference fuels. The authors also wish to thank Glyn Davies and Mike Braisher of Jaguar Land Rover for their assistance in undertaking the transient dynamometer experiments.

Funding

This work was supported by the Engineering and Physical Sciences Research Council and Jaguar Land Rover.

References

1. Zhao H. Overview of Gasoline Direct Injection Engines. *Advanced direct injection combustion engine technologies and development: Gasoline and gas engines*. Woodhead Publishing Ltd, 2010.
2. Braisher, M., Stone, R., and Price, P., "Particle Number Emissions from a Range of European Vehicles," SAE Technical Paper 2010-01-0786, 2010, doi:10.4271/2010-01-0786.
3. Commission Regulation 692/2008, OJ L 199 of 18.7.2008.
4. Aikawa K, Sakurai T and Jetter JJ. Development of a Predictive Model for Gasoline Vehicle Particulate Matter Emissions. *SAE International Journal of Fuels and Lubricants*. 2010; 3: 610-22.
5. Aikawa K and Jetter JJ. Impact of gasoline composition on particulate matter emissions from a direct-injection gasoline engine: Applicability of the particulate matter index. *International Journal of Engine Research*. 2014; 15: 298-306.
6. Andersson J, Giechaskiel B, Muñoz-Bueno R, Sandbach E and Dilara P. Particle Measurement Programme (PMP) Light-duty Inter-laboratory Correlation Exercise (ILCE_LD) Final Report. European Commission Joint Research Centre Institute for Environment and Sustainability, 2007.
7. Commission Regulation 692/2008, OJ L 199 of 18.7.2008, p.88.
8. Sandford, M., Page, G., and Crawford, P., "The All New AJV8," SAE Technical Paper 2009-01-1060, 2009, doi:10.4271/2009-01-1060.
9. Peckham, M., Finch, A., Campbell, B., Price, P. et al., "Study of Particle Number Emissions from a Turbocharged Gasoline Direct Injection (GDI) Engine Including Data from a Fast-Response Particle Size Spectrometer," SAE Technical Paper 2011-01-1224, 2011, doi:10.4271/2011-01-1224.
10. Chen, L., Braisher, M., Crossley, A., Stone, R. et al., "The Influence of Ethanol Blends on Particulate Matter Emissions from Gasoline Direct Injection Engines," SAE Technical Paper 2010-01-0793, 2010, doi:10.4271/2010-01-0793.
11. Reavell, K., Hands, T., and Collings, N., "A Fast Response Particulate Spectrometer for Combustion Aerosols," SAE Technical Paper 2002-01-2714, 2002, doi:10.4271/2002-01-2714.
12. Braisher, M. *Particulate Matter Emissions Measurements from Engines and Vehicles*. DPhil thesis. University of Oxford, 2010, p.80. Also published in [2].
13. Giechaskiel B, Cresnoverh M, Jörgl H and Bergmann A. Calibration and accuracy of a particle number measurement system. *Measurement Science and Technology*. 2010; 21: 045102.
14. Cheng WK, Summers T and Collings N. The fast-response flame ionization detector. *Progress in Energy and Combustion Science*. 1998; 24: 89-124.
15. Reid RC, Prausnitz JM and Poling BE. *The properties of gases and liquids*. 4th ed. New York ; London: McGraw-Hill, 1987, p.x, 741 p.
16. Vidal J. *Thermodynamics: Applications in Chemical Engineering and the Petroleum Industry*. Editions OPHRYS, 2003, p.492.
17. Fredenslund A and Gmehling. *Vapor-Liquid equilibrium using UNIFAC a group-contribution method*. Elsevier North-Holland Inc., 1977.
18. EN 13016:2007. Liquid petroleum products. Vapour pressure. Determination of air saturated vapour pressure (ASVP) and calculated dry vapour pressure equivalent (DVPE).
19. Atkins PW. *Physical Chemistry*. 5th ed.: Oxford University Press, 1994.
20. EN228:2008 Automotive fuels. Unleaded petrol. Requirements and test methods. 2008.
21. Abrams DS and Prausnitz JM. Statistical thermodynamics of liquid mixtures: A new expression for the excess Gibbs energy of partly or completely miscible systems. *AIChE Journal*. 1975; 21: 116-28.
22. Poling BE, Reid RC, Prausnitz JM and O'Connell JP. *The properties of gases and liquids*. 5th ed. New York ; London: McGraw-Hill, 2001, p.ix, [789] p.

Appendix 1

Notation

AFR	Air Fuel Ratio
APC	AVL Particle Counter
ASVP	Air Saturated Vapour Pressure
BMEP	Brake Mean Effective Pressure
CA bTDC	Crank Angle before Top Dead Centre
DBE	Double Bond Equivalent
DHA	Detailed Hydrocarbon Analysis
DISI	Direct Injection Spark Ignition
DMS	Differential Mobility Spectrometer
DVPE	Dry Vapour Pressure Equivalent
EU	European Union
FBP	Final Boiling Point
fFID	Fast Flame Ionisation Detector
GDI	Gasoline Direct Injection
IMEP	Indicated Mean Effective Pressure
NEDC	New European Drive Cycle
PFI	Port Fuel Injection
PM	Particulate Matter
PMP	Particle Measurement Programme
PN	Particle Number
RON	Research Octane Number
RVP	Reid Vapour Pressure
SGDI	Spray Guided Direct Injection
TWC	Three Way Catalyst
UNIFAC	UNiversal Functional Activity Coefficient
VP	Vapour Pressure
λ	Ratio of actual Air Fuel Ratio to Stoichiometric Air Fuel Ratio
ΔH_{vap}	Latent heat of vaporisation

Appendix 2

The UNIFAC method (UNIFAC) was proposed by Fredenslund et al¹⁸, so as to extend Raoult's Law to account for non-ideal mixing. It combines the Analytical Solution of Groups (ASOG) method, relating activity coefficients to molecular structural group interactions, with the UNIQUAC (UNIFAC QUAsiChemical) model²¹. It is a semi-empirical model to predict non-ideal mixture behaviour based on molecular size and known interactions. It breaks molecules into functional groups to model interactions using empirical data from experimentally determined interactions.

The model essentially breaks down into two parts: the combinatorial part, due to the differences in size and shape of the molecules; and the residual part, due to energy interactions.

The UNIFAC equations are shown below²²:

$$\ln \gamma_i = \ln \gamma_i^C + \ln \gamma_i^R$$

$$\ln \gamma_i^C = \ln \frac{\Phi_i}{x_i} + \frac{z}{2} q_i \ln \frac{\theta_i}{\Phi_i} + l_i - \frac{\Phi_i}{x_i} \sum x_j l_j$$

$$\ln \gamma_i^R = \sum_k v_k^{(i)} (\ln \Gamma_k - \ln \Gamma_k^{(i)})$$

$$\ln \Gamma_k = Q_k \left[1 - \ln \left(\sum_m \theta_m \psi_{mk} \right) - \sum_m \frac{\theta_m \psi_{km}}{\sum_n \theta_n \psi_{nm}} \right]$$

$$l_i = \frac{z}{2} (r_i - q_i) - (r_i - 1)$$

$$\theta_i = \frac{q_i x_i}{\sum_j q_j x_j}$$

$$\psi_{mn} = \exp \left(-\frac{a_{mn}}{T} \right)$$

$$\Phi_i = \frac{r_i x_i}{\sum_j r_j x_j}$$

$$r_i = \sum_k v_k^{(i)} R_k$$

$$q_i = \sum_k v_k^{(i)} Q_k$$

x_i is the molar fraction of component i

θ_i is the area fraction

Φ_i is the segment fraction

r_i is the normalised molecular Van der Waals volume

q_i is the normalised molecular surface area

Γ_k is the group residual activity coefficient and $\Gamma_k^{(i)}$ is the same in a solution only of molecules of type i

$v_k^{(i)}$ is the number of groups of type k in the molecule i

Appendix 3

Table 9: Model test fuel composition

Fuel	Light components	Medium components			Heavy components			DBE+1	VP ¹ (kPa)	PM index ²	PN index
% v/v	n-pentane	iso-octane	n-octane	Toluene	iso-decane ³	n-decane	TMB ⁴				(×100)
T0	5.00	71.25	23.75	0.00	0.00	0.00	0.00	1.00	15.37	0.341	6.51
T25	5.00	53.44	17.81	23.75	0.00	0.00	0.00	1.95	15.73	0.511	12.40
T35 ⁵	5.00	46.31	15.44	33.25	0.00	0.00	0.00	2.33	15.55	0.615	14.99
T42	5.00	41.32	13.78	39.90	0.00	0.00	0.00	2.60	15.41	0.684	18.50
T50	5.00	35.63	11.88	47.5	0.00	0.00	0.00	2.90	15.27	0.762	19.00
T75	5.00	17.81	5.94	71.25	0.00	0.00	0.00	3.85	14.75	0.987	26.09
T100	5.00	0.00	0.00	95.00	0.00	0.00	0.00	4.80	14.08	1.19	34.08
D0 ⁵	5.00	46.31	15.44	33.25	0.00	0.00	0.00	2.33	15.55	0.615	14.99
D10	5.00	41.68	13.89	29.93	1.48	4.69	3.33	2.33	14.92	0.789	15.62
D20	5.00	37.05	12.35	26.60	2.96	9.37	6.65	2.33	14.26	0.962	16.34
D30	5.00	32.42	10.81	23.28	4.45	14.08	9.98	2.33	13.56	1.13	17.18
D40	5.00	27.79	9.26	19.95	5.93	18.77	13.30	2.33	12.84	1.31	18.15
D0*	0.00	48.75	16.25	35.00	0.00	0.00	0.00	2.40	9.51	0.408	25.25
D10*	0.00	43.88	14.63	31.50	1.56	4.94	3.50	2.40	8.76	0.541	27.40
D20*	0.00	39.00	13.00	28.00	3.12	9.88	7.00	2.40	7.98	0.674	30.09
D30*	0.00	34.13	11.38	24.50	4.68	14.82	10.50	2.40	7.16	0.806	33.53
D40*	0.00	29.25	9.75	21.00	6.24	19.76	14.00	2.40	6.31	0.937	38.06

1. VP is estimated according to the UNIFAC model, not calculated

2. PM index calculated by % mass as in Aikawa et al⁴

3. 2,2,3,3-tetramethylhexane

4. 1,3,5-trimethylbenzene

5. N.B. T35 ≡ D0

A star (*) indicates a fuel with the same composition as an unstarred fuel, but without 5% v/v n-pentane